University of Reading

Force-free collisionless current sheet models with non-uniform temperature and density profiles

Article

Published Version

Creative Commons: Attribution 4.0 (CC-BY)

Open access

Wilson, F., Neukirch, T. and Allanson, O. (2017) Force-free collisionless current sheet models with non-uniform temperature and density profiles. Physics of Plasmas, 24 (9). 092105. ISSN 1070-664X doi: 10.1063/1.4997703 Available at https://centaur.reading.ac.uk/72309/

It is advisable to refer to the publisher's version if you intend to cite from the work. See Guidance on citing.
Published version at: http://dx.doi.org/10.1063/1.4997703
To link to this article DOI: http://dx.doi.org/10.1063/1.4997703

Publisher: AIP Publishing

All outputs in CentAUR are protected by Intellectual Property Rights law, including copyright law. Copyright and IPR is retained by the creators or other copyright holders. Terms and conditions for use of this material are defined in the End User Agreement.

www.reading.ac.uk/centaur

CentAUR

University of Reading

Central Archive at the University of Reading

Reading's research outputs online

Force-free collisionless current sheet models with non-uniform temperature and density profiles

F. Wilson, , T. Neukirch, and , and O. Allanson

Citation: Physics of Plasmas **24**, 092105 (2017); doi: 10.1063/1.4997703
View online: http://dx.doi.org/10.1063/1.4997703
View Table of Contents: http://aip.scitation.org/toc/php/24/9
Published by the American Institute of Physics

Force-free collisionless current sheet models with non-uniform temperature and density profiles

F. Wilson,[1,a)] T. Neukirch,[1] and O. Allanson[1,2]
[1]*School of Mathematics and Statistics, University of St. Andrews, St. Andrews KY16 9SS, United Kingdom*
[2]*Space and Atmospheric Electricity Group, Department of Meteorology, University of Reading, Reading RG6 6BB, United Kingdom*

(Received 26 July 2017; accepted 2 August 2017; published online 17 August 2017)

We present a class of one-dimensional, strictly neutral, Vlasov-Maxwell equilibrium distribution functions for force-free current sheets, with magnetic fields defined in terms of Jacobian elliptic functions, extending the results of Abraham-Shrauner [Phys. Plasmas **20**, 102117 (2013)] to allow for non-uniform density and temperature profiles. To achieve this, we use an approach previously applied to the force-free Harris sheet by Kolotkov *et al.* [Phys. Plasmas **22**, 112902 (2015)]. In one limit of the parameters, we recover the model of Kolotkov *et al.* [Phys. Plasmas **22**, 112902 (2015)], while another limit gives a linear force-free field. We discuss conditions on the parameters such that the distribution functions are always positive and give expressions for the pressure, density, temperature, and bulk-flow velocities of the equilibrium, discussing the differences from previous models. We also present some illustrative plots of the distribution function in velocity space.
© 2017 Author(s). All article content, except where otherwise noted, is licensed under a Creative Commons Attribution (CC BY) license (http://creativecommons.org/licenses/by/4.0/).
[http://dx.doi.org/10.1063/1.4997703]

I. INTRODUCTION

Force-free current sheets, with magnetic fields satisfying

$$\nabla \cdot \mathbf{B} = 0, \tag{1}$$

$$\nabla \times \mathbf{B} = \mu_0 \mathbf{j}, \tag{2}$$

$$\mathbf{j} \times \mathbf{B} = 0, \tag{3}$$

are appropriate for plasma modelling in, e.g., the solar atmosphere and planetary magnetospheres (e.g., Refs. 3–15). Equations (1)–(3) imply that the current density is parallel to the magnetic field: $\mathbf{j} = \alpha(\mathbf{r})\mathbf{B}$. The case where $\alpha = 0$ defines a potential field, and when α is constant, we have a linear force-free field. When α varies with the position $\mathbf{r}$, the field is referred to as nonlinear force-free.

Such current sheets as described earlier can play a crucial role in, e.g., magnetic reconnection processes, for which it is often necessary to consider kinetic length scales (e.g., Ref. 16), since many astrophysical plasmas are approximately collisionless. To initialise the studies of collisionless reconnection, a Vlasov-Maxwell (VM) equilibrium can be used; since current sheets are strongly localised, they are often well described by one-dimensional (1D) VM equilibrium models. The work by Wilson *et al.*[17] was the first example of a study of collisionless reconnection for which an exact nonlinear force-free equilibrium was used in the initial setup, using a distribution function (DF) found by Harrison and Neukirch[18] for the "force-free Harris" current sheet

$$\mathbf{B} = B_0(\tanh(z/L), \operatorname{sech}(z/L), 0). \tag{4}$$

Other studies of collisionless reconnection in force-free current sheets have involved the use of approximate force-free equilibria (e.g., Refs. 19–26) or linear force-free equilibria (e.g., Refs. 27–29).

To find VM equilibrium DFs consistent with force-free current sheets involves solving the VM equations in the opposite order from what is usually done; a magnetic field satisfying Equations (1)–(3) is specified, and the DFs are then given by the solution of an inverse problem (e.g., Refs. 30–33). As such, finding exact force-free VM equilibria is generally a non-trivial task, and this is reflected in the relatively small number of known solutions. Linear force-free VM equilibria have been discussed in, e.g., Refs. 18, 27, 31, and 34–37. The first solution for a nonlinear force-free field was found by Harrison and Neukirch[38] (see also Ref. 39) for the force-free Harris sheet, and these solutions were later extended by Kolotkov *et al.*[2] to allow for non-uniform density and temperature profiles (with respect to the spatial coordinate). A number of other equilibrium DFs have also been found for this field. Wilson and Neukirch[40] found DFs with an arbitrary dependence on the particle energy; Stark and Neukirch[41] discussed DFs in the relativistic limit; Allanson *et al.*[33,42] found DFs in terms of infinite sums over Hermite polynomials, with an arbitrarily low plasma beta (in the previous work on the force-free Harris sheet, the plasma beta was constrained to be greater than unity); Dorville *et al.*[43] discussed "semi-analytic" DFs for a magnetic field, which includes the force-free Harris sheet as a special case.

Abraham-Shrauner[1] discussed VM equilibria for a nonlinear force-free magnetic field given in terms of Jacobian elliptic functions. This work can be thought of as a generalisation of some of the previous work, to account for both linear and nonlinear force-free equilibria in one model, since,

[a)]Electronic mail: fw237@st-andrews.ac.uk

 © Author(s) 2017.

in one limit of the elliptic modulus, the magnetic field becomes the force-free Harris sheet field, and in another limit, it becomes a linear force-free field. The DFs discussed give rise to spatially uniform temperature and density profiles, in a similar way to some of the models mentioned above. In this paper, we will extend this class of DFs to include those consistent with non-uniform temperature and density profiles, using a similar approach used by Kolotkov *et al.*[2] for the force-free Harris sheet. As for Abraham-Shrauner's DFs, the new DFs we will discuss include both the linear force-free limit and the force-free Harris sheet limit.[2]

The paper is laid out as follows; in Sec. II, we outline the background theory of 1D VM equilibria; in Sec. III, we present an overview of the work by Abraham-Shrauner;[1] we discuss the extension of this work to include non-uniform temperature and density profiles in Sec. IV, and the velocity space structure of the new DFs is discussed in Sec. V; we end with a summary in Sec. VI.

II. 1D VLASOV-MAXWELL EQUILIBRIA

In line with some of the previous work on 1D VM equilibria (e.g., Refs. 18, 38, and 39), we assume that all quantities depend only on the z-coordinate and that the magnetic field, $\mathbf{B} = (B_x, B_y, 0)$, can be written as the curl of a vector potential, $\mathbf{A} = (A_x, A_y, 0)$. We will not repeat all of the details here, but the result of the above assumptions is that the problem reduces to solving Ampère's law in the form

$$\frac{\mathrm{d}^2 A_x}{\mathrm{d}z^2} = -\mu_0 \frac{\partial P_{zz}}{\partial A_x}, \tag{5}$$

$$\frac{\mathrm{d}^2 A_y}{\mathrm{d}z^2} = -\mu_0 \frac{\partial P_{zz}}{\partial A_y}, \tag{6}$$

to find P_{zz}, which is the zz-component of the pressure tensor, defined by

$$P_{zz}(A_x, A_y) = \sum_s m_s \int v_z^2 f_s(H_s, p_{xs}, p_{ys}) \mathrm{d}^3 v, \tag{7}$$

where we assume that the DFs can be chosen in such a way that they are compatible with strict neutrality (the scalar potential $\phi = 0$).[31] Note that we only consider P_{zz} since this is the component of the pressure tensor which is important for the force-balance of the 1D equilibrium. The DFs, denoted by f_s, are assumed to be functions of the particle energy, $H_s = m_s(v_x^2 + v_y^2 + v_z^2)/2$, and the x- and y-components of the canonical momentum, $\mathbf{p} = m_s\mathbf{v} + q_s\mathbf{A}$, since these are known constants of motion for a time-independent system with spatial invariance in the x- and y-directions. Once Ampère's law has been solved for P_{zz}, the DF can be found by solving Eq. (7). This is an example of an inverse problem.

III. ABRAHAM-SHRAUNER'S MODEL

In this section, we discuss some properties of the model developed by Abraham-Shrauner,[1] in order to give context to the discussion we will present in Sec. IV. In Abraham-Shrauner's work, a nonlinear force-free current sheet profile is considered, described by the magnetic field

$$\mathbf{B} = B_0(\mathrm{sn}(z/L), \mathrm{cn}(z/L), 0), \tag{8}$$

where B_0 is a constant, L is the current sheet half-thickness, and sn and cn are Jacobian elliptic functions[44] with the modulus k suppressed (where $0 \leq k \leq 1$). In the limit $k \to 0$, $\mathrm{sn}(z/L) \to \sin(z/L)$ and $\mathrm{cn}(z/L) \to \cos(z/L)$, and so the magnetic field (8) becomes the linear force-free field $\mathbf{B} = B_0(\sin(z/L), \cos(z/L), 0)$. In the limit $k \to 1$, $\mathrm{sn}(z/L) \to \tanh(z/L)$ and $\mathrm{cn}(z/L) \to \mathrm{sech}(z/L)$, giving the force-free Harris sheet magnetic field [Eq. (4)]. The vector potential, $\mathbf{A}$, used by Abraham-Shrauner[1] is given by

$$A_x = \frac{B_0 L}{k}\left(\arcsin(k\,\mathrm{sn}(z/L)) + \frac{k\pi}{2}\right), \tag{9}$$

$$A_y = \frac{B_0 L}{k}\ln\left(\frac{k\,\mathrm{cn}(z/L) + \mathrm{dn}(z/L)}{1+k}\right), \tag{10}$$

where dn is also an elliptic function. This can be seen by using standard integrals[45] and by choosing the integration constants such that, when $k \to 1$, $A_x \to 2B_0 L \arctan(e^{z/L})$, $A_y \to -\ln(\cosh(z/L))$—the vector potential components used in some of the previous work on the force-free Harris sheet (note also that an alternative gauge for $\mathbf{A}$ is discussed for the force-free Harris sheet by Allanson *et al.*[33]).

The current density is given by

$$\mathbf{j} = \frac{B_0}{\mu_0 L}(\mathrm{sn}(z/L)\mathrm{dn}(z/L), \mathrm{cn}(z/L)\mathrm{dn}(z/L), 0) = \frac{\mathrm{dn}(z/L)\mathbf{B}}{\mu_0 L}, \tag{11}$$

and so the force-free parameter α is given by

$$\alpha(z) = \frac{\mathrm{dn}(z/L)}{\mu_0 L}. \tag{12}$$

Note that, in the limit $k \to 0$, $\mathrm{dn}(z/L) \to 1$, and so α is constant (the linear force-free case), but is otherwise a function of position (the nonlinear force-free case).

It is assumed that the pressure has the form $P_{zz}(A_x, A_y) = P_1(A_x) + P_2(A_y)$; Ampère's law in the form of Eqs. (5) and (6) can then be solved for P_{zz} in terms of the macroscopic parameters, which gives

$$\begin{aligned} P_{zz} = {} & P_{t1} + P_{t2} \\ & - \frac{B_0^2}{2\mu_0}\left(\frac{3}{2} + \frac{1}{2k^2}\cos\left(\frac{2kA_x}{B_0 L} - k\pi\right)\right. \\ & \left. - \frac{1}{4}\left(\frac{1}{k}+1\right)^2 \exp\left(\frac{2kA_y}{B_0 L}\right) - \frac{1}{4}\left(\frac{1}{k}-1\right)^2 \exp\left(-\frac{2kA_y}{B_0 L}\right)\right), \end{aligned} \tag{13}$$

where P_{t1} and P_{t2} are constants. This expression can then be used in Eq. (7) to determine the DF, which can be written in terms of the constants of motion as

$$f_s(H_s,p_{xs},p_{ys}) = \frac{n_{0s}e^{-\beta_s H_s}}{\left(\sqrt{2\pi}v_{th,s}\right)^3}\left[a_{0s} - \frac{1}{2k^2}\exp\left(\frac{(1+k^2)u_{ys}^2}{2v_{th,s}^2}\right)\right.$$
$$\times\cos\left(k\beta_s u_{xs}p_{xs} - k\pi\right) + \frac{1}{4}\left(\frac{1}{k}+1\right)^2$$
$$\times\exp\left(\frac{(1-k^2)u_{ys}^2}{2v_{th,s}^2}\right)\exp\left(k\beta_s u_{ys}p_{ys}\right)$$
$$+\frac{1}{4}\left(\frac{1}{k}-1\right)^2\exp\left(\frac{(1-k^2)u_{ys}^2}{2v_{th,s}^2}\right)$$
$$\left.\times\exp\left(-k\beta_s u_{ys}p_{ys}\right)\right], \tag{14}$$

where a_{0s} is a dimensionless constant, u_{xs} and u_{ys} are constant parameters with the dimension of velocity, $\beta_s = (k_B T_s)^{-1}$ and $v_{th,s} = (\beta_s m_s)^{-1/2}$. In the limit $k \to 1$, this DF takes the form of that discussed in Refs. 38 and 39 for the force-free Harris sheet. In the opposite limit, i.e., $k \to 0$, it takes a general form which is similar to that described in Refs. 18, 31, and 37, but with a shift in p_{xs} and p_{ys} (this corresponds to a regauging of the vector potential).

Note that a number of relations exist between the parameters of the model, to ensure positivity of the DFs, strict neutrality, and consistency between the microscopic and macroscopic descriptions of the equilibrium (see Ref. 1 for further details). Using these relations, the equilibrium density, pressure, and temperature can be expressed as

$$n = n_0\left(a_0 + \frac{1}{2}\right), \tag{15}$$

$$P_{zz} = \frac{n_0(\beta_e+\beta_i)}{\beta_e\beta_i}\left(a_0+\frac{1}{2}\right), \tag{16}$$

$$T = \frac{P_{zz}}{n} = \frac{\beta_e+\beta_i}{\beta_e\beta_i}, \tag{17}$$

where a_0 and n_0 are constant parameters that are introduced when the strict neutrality condition ($\phi = 0$) is imposed. The expressions (15)–(17) are independent of the elliptic modulus k; this can be seen for P_{zz} through the force-balance equation

$$\frac{B^2}{2\mu_0} + P_{zz} = P_T, \tag{18}$$

where P_T is the total pressure, since $B^2 = |\mathbf{B}|^2 = B_0^2$ for the magnetic field (8), which is independent of k. Since, in this case, $P_{zz} = (\beta_e+\beta_i)n/(\beta_e\beta_i)$, it follows that the density and temperature will also be independent of k. As can be seen from the expressions (15) and (17), Abraham-Shrauner's model has density and temperature profiles that are constant across the current sheet, in a similar way to the models discussed in Refs. 18, 33, and 38–42. In Sec. IV, we discuss how the method of Kolotkov *et al.*[2] can be used to extend the model to have spatially non-uniform density and temperature profiles across the current sheet, while still maintaining a constant pressure as is required for a force-free equilibrium (see, e.g., Ref. 18).

IV. EXTENSION TO NON-UNIFORM TEMPERATURE/DENSITY CASE

To extend the model of Abraham-Shrauner[1] to have non-uniform temperature and density profiles, we consider a DF of the form

$$f_s = \frac{n_{0s}\gamma^{3/2}}{\left(\sqrt{2\pi}v_{th,s}\right)^3}\exp\left(-\gamma\beta_s H_s\right)\left(a_{0s}+a_{1s}\cos\left(\gamma k\beta_s u_{xs}p_{xs}-k\pi\right)\right)$$
$$+\frac{n_{0s}}{\left(\sqrt{2\pi}v_{th,s}\right)^3}\exp\left(-\beta_s H_s\right)\left(b_{0s}+b_{1s}\exp\left(k\beta_s u_{ys}p_{ys}\right)\right.$$
$$\left.+b_{2s}\exp\left(-k\beta_s u_{ys}p_{ys}\right)\right), \tag{19}$$

(where $\gamma > 0$) i.e., a modification of Abraham-Shrauner's DF. This corresponds to assuming that the p_{xs}-dependent population has a different energy dependence than the p_{ys}-dependent population, through the factor γ. We effectively also have two separate constant background populations (through the constants a_{0s} and b_{0s}) whose energy dependences differ. These two populations have been included to allow the limit $k \to 0$ to exist, and to ensure this we assume that the constants a_{0s} and b_{0s} scale with the elliptic modulus k as follows:

$$a_{0s} = \bar{a}_{0s} + \frac{\gamma}{2k^2}\exp\left(\frac{u_{xs}^2}{2v_{th,s}^2}\right), \tag{20}$$

$$b_{0s} = \bar{b}_{0s} - \frac{1}{2k^2}\exp\left(\frac{u_{xs}^2}{2v_{th,s}^2}\right), \tag{21}$$

for constants $\bar{a}_{0s}$ and $\bar{b}_{0s}$. Note that we have defined the constants in this way so that we have a model that works for all k values between 0 and 1, but for finite small k (or large $u_{xs}/v_{th,s}$), the k-dependent parts of a_{0s} and b_{0s} can become very large, which may lead to, e.g., a large maximum density, which may not be physically appropriate. If we were only interested in a particular finite small value of k, we could redefine the constants to avoid such issues.

By calculating the number density ($n_s = \int f_s \mathrm{d}^3 v$) of the modified DF (19), and imposing the condition $\phi = 0$ ($n_i(A_x,A_y) = n_e(A_x,A_y)$), we obtain the neutrality relations (A1)–(A8) in the Appendix. We can then express $n_s = n$ as

$$n(A_x,A_y) = n_0[a_0+b_0+a_1\cos\left(\gamma k\beta_s u_{xs}q_s A_x - k\pi\right)$$
$$+b_1\exp\left(k\beta_s u_{ys}q_s A_y\right)+b_2\exp\left(-k\beta_s u_{ys}q_s A_y\right)], \tag{22}$$

and the pressure can be calculated from the DF through Eq. (7) as

$$P_{zz} = n_0\frac{\beta_e+\beta_i}{\beta_e\beta_i}\left(\frac{a_0}{\gamma}+b_0+\frac{a_1}{\gamma}\cos\left(\gamma k\beta_s u_{xs}q_s A_x - k\pi\right)\right.$$
$$\left.+b_1\exp\left(k\beta_s u_{ys}q_s A_y\right)+b_2\exp\left(-k\beta_s u_{ys}q_s A_y\right)\right). \tag{23}$$

Note the γ^{-1} factors appearing in parts of Eq. (23), meaning that the pressure is no longer simply a multiple of the density

as in Abraham-Shrauner's model. Eq. (23) for the pressure can be compared with Eq. (13) to give the relations (A11)–(A16) (see the Appendix) between the microscopic and macroscopic parameters. Using these relations, and the neutrality relations in the Appendix, the modified DF (19) can then be written as

$$f_s = \frac{\gamma^{3/2} n_{0s} \exp\left(-\gamma\beta_s H_s\right)}{\left(\sqrt{2\pi} v_{th,s}\right)^3} \left(a_{0s} - \frac{\gamma}{2k^2} \exp\left(\frac{\left(\gamma k^2 + 1\right) u_{xs}^2}{2 v_{th,s}^2} \right) \times \cos\left(\gamma k \beta_s u_{xs} p_{xs} - k\pi\right) \right) + \frac{n_{0s} \exp\left(-\beta_s H_s\right)}{\left(\sqrt{2\pi} v_{th,s}\right)^3} \left(\frac{1}{4} \exp\left(\frac{u_{xs}^2 - k^2 u_{ys}^2}{2 v_{th,s}^2} \right) \times \left\{ \left(\frac{1}{k} + 1 \right)^2 \exp\left(k \beta_s u_{ys} p_{ys}\right) + \left(\frac{1}{k} - 1 \right)^2 \exp\left(-k \beta_s u_{ys} p_{ys}\right) \right\} + b_{0s} \right). \tag{24}$$

Sufficient conditions for the positivity of the DF (24) across the whole phase space can be derived by assuming that the functions

$$g_{1s}(p_{xs}) = a_{0s} - \frac{\gamma}{2k^2} \exp\left(\frac{\left(\gamma k^2 + 1\right) u_{xs}^2}{2 v_{th,s}^2} \right) \cos\left(\gamma k \beta_s u_{xs} p_{xs} - k\pi\right), \tag{25}$$

$$g_{2s}(p_{ys}) = b_{0s} + \frac{1}{4} \exp\left(\frac{u_{xs}^2 - k^2 u_{ys}^2}{2 v_{th,s}^2} \right) \times \left(\left(\frac{1}{k} + 1 \right)^2 \exp\left(k \beta_s u_{ys} p_{ys}\right) + \left(\frac{1}{k} - 1 \right)^2 \exp\left(-k \beta_s u_{ys} p_{ys}\right) \right), \tag{26}$$

are both positive, and are given by

$$\bar{a}_0 > \frac{\gamma}{2k^2} \left[\exp\left(\frac{\gamma k^2 u_{xs}^2}{2 v_{th,s}^2} \right) - 1 \right], \tag{27}$$

$$\bar{b}_0 > \frac{1}{2k^2} \left[1 - (1 - k^2) \exp\left(- \frac{k^2 u_{ys}^2}{2 v_{th,s}^2} \right) \right], \tag{28}$$

where $\bar{a}_0$ and $\bar{b}_0$ are defined in the Appendix. Note that these conditions are well defined in the limit $k \to 0$. Since $0 \le k \le 1$, $\gamma > 0$ and the exponential term in Eq. (27) has a minimum value of unity, we see that $\bar{a}_0 \ge 0$.

The new DF (24) describes an equilibrium with non-uniform density and temperature profiles; we can show this by writing them as functions of z using Eqs. (9), (10), and (A13)–(A15) and the definitions of $\bar{a}_0$ and $\bar{b}_0$, which gives

$$n(z) = n_0 \left[\bar{a}_0 + \bar{b}_0 + \frac{1}{2} + (\gamma - 1) \mathrm{sn}^2(z/L) \right], \tag{29}$$

$$T(z) = \frac{P_{zz}}{n} = \frac{\beta_e + \beta_i}{\beta_e \beta_i} \left(\frac{\bar{a}_0}{\gamma} + \bar{b}_0 + \frac{1}{2} \right) \left(\bar{a}_0 + \bar{b}_0 + \frac{1}{2} + (\gamma - 1) \mathrm{sn}^2(z/L) \right)^{-1}, \tag{30}$$

where the uniform value of the pressure is given by

$$P_{zz} = \frac{n_0 (\beta_e + \beta_i)}{\beta_e \beta_i} \left(\frac{\bar{a}_0}{\gamma} + \bar{b}_0 + \frac{1}{2} \right), \tag{31}$$

which is independent of the modulus k (for the same reasons as discussed in Sec. III), and is similar to the expression found by Kolotkov *et al.*[2] for the force-free Harris sheet. Note, however, that this time the density depends on k, due to the introduction of the γ factors in the DF (the pressure can no longer be written as $P_{zz} = (\beta_e + \beta_i) n / (\beta_e \beta_i)$ as it can in the uniform temperature model). It can be seen that, for $\gamma = 1$, we recover the constant density/temperature case of Abraham-Shrauner.[1]

Provided the DF (24) is positive over the whole phase space, then the density, pressure, and temperature will also be positive everywhere. Note, however, that the opposite is not true, i.e., a positive density and pressure do not imply a positive DF. We ensure that the DF is positive by choosing parameters in such a way that the conditions (27) and (28) are satisfied (for both ions and electrons). Figure 1 shows profiles of the density and temperature for different values of γ, with $k = 0$ (the linear force-free case). Figure 2 shows the same quantities with $k = 0.5$. They are normalised to have a value of unity at the lower z-boundary of each plot, and we have chosen parameters such that the DFs are positive for ions and electrons (note that if we choose $u_{xe}/v_{th,e}$, then this fixes $u_{xi}/v_{th,i}$ through Eq. (A7), if we specify the mass ratio and the ratio β_e/β_i). For $\gamma = 1.0$ in each figure, we see that both the density and temperature are constant, as in Abraham-Shrauner's model. For the other values of γ shown, the quantities have a periodic structure. In regions where the density is enhanced/depleted (with respect to the constant value for $\gamma = 1$), there is a corresponding depletion/enhancement of the temperature, which ensures that the two quantities multiply together to give a constant pressure, as required for the force-free equilibrium. Additionally, in regions where the values of $\gamma > 1$ lead to an enhancement/depletion of the quantities, the opposite behaviour is seen when $\gamma < 1$, i.e., a depletion/enhancement of the quantities. Similar features are seen by Kolotkov *et al.*[2] (which we obtain in the limit $k \to 1$), but note that the density and temperature are not periodic in this case, and so, for a particular γ value, there is either an enhancement or depletion of the density/temperature (not both).

We will now briefly discuss some other properties of the model. The plasma beta, defined in this case as the ratio of P_{zz} to the magnetic pressure $B_0^2/(2\mu_0)$, is given [using Eq. (A11)] by

$$\beta_{pl} = \frac{\bar{a}_0}{\gamma} + \bar{b}_0 + \frac{1}{2}. \tag{32}$$

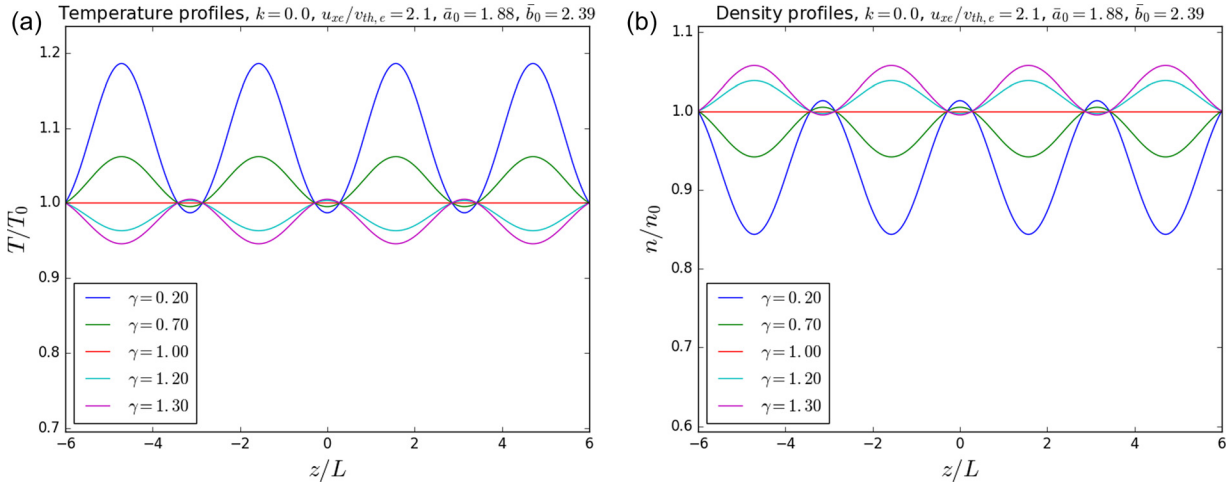

FIG. 1. (a) Density and (b) temperature profiles for various values of γ, for $k=0$ (the linear force-free case). Both quantities are normalised to have a value of unity at the lower z-boundary.

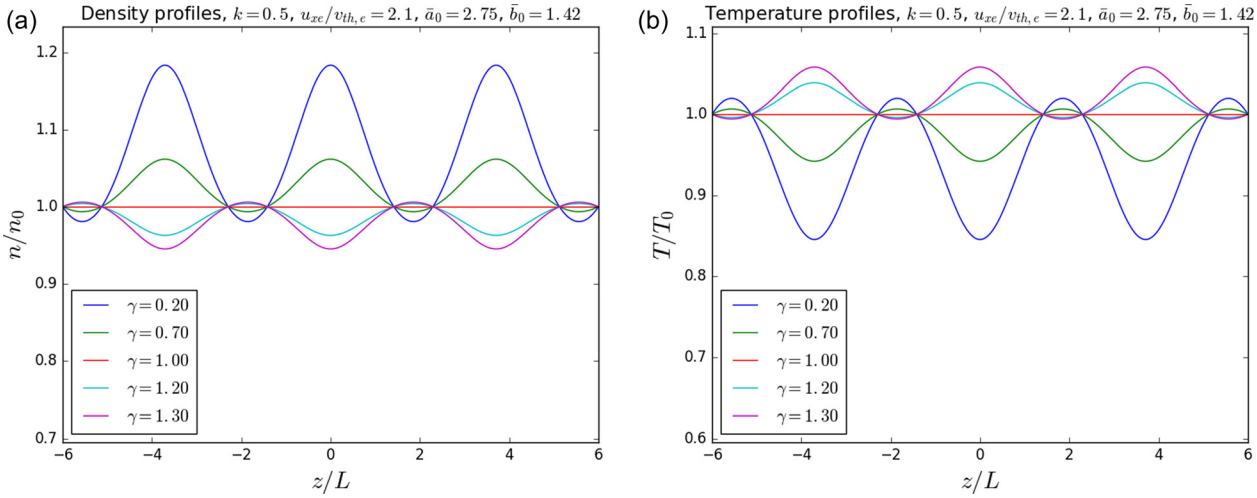

FIG. 2. (a) Density and (b) temperature profiles for various values of γ, for $k=0.5$. Both quantities are normalised to have a value of unity at the lower z-boundary.

Using the conditions (27) and (28) for positivity of the DF, we have that

$$\beta_{pl} > \frac{1}{2} + \frac{1}{2k^2}\left[\exp\left(\frac{\gamma k^2 u_{xs}^2}{2v_{th,s}^2}\right) - (1-k^2)\exp\left(-\frac{k^2 u_{ys}^2}{2v_{th,s}^2}\right)\right]. \tag{33}$$

For $k=0$ and $k=1$, for example, it is straightforward to show that β_{pl} must be greater than unity (as in, e.g., the models in Refs. 1, 2, 38, and 40), since $u_{xs}^2/v_{th,s}^2 \geq 0$.

The bulk-flow velocity components, defined by

$$\mathbf{V}_s = \frac{1}{n_s}\int \mathbf{v} f_s \mathrm{d}^3 v, \tag{34}$$

have the form

$$V_{xs} = \frac{\gamma u_{xs}\mathrm{sn}(z/L)\mathrm{dn}(z/L)}{\bar{a}_0 + \bar{b}_0 + 1/2 + (\gamma-1)\mathrm{sn}^2(z/L)}, \tag{35}$$

$$V_{ys} = \frac{u_{ys}\mathrm{cn}(z/L)\mathrm{dn}(z/L)}{\bar{a}_0 + \bar{b}_0 + 1/2 + (\gamma-1)\mathrm{sn}^2(z/L)}, \tag{36}$$

$$V_{zs} = 0. \tag{37}$$

Through these expressions, we see the role played by the parameters u_{xs} and u_{ys}, which can also be written in terms of the ratio of the species gyroradius, $r_{g,s}$, to the current sheet half-width, L, by using Eq. (A16) (similarly to Neukirch *et al.*[39]) as

$$\frac{u_{ys}^2}{v_{th,s}^2} = \frac{\gamma^2 u_{xs}^2}{v_{th,s}^2} = 4\frac{r_{g,s}^2}{L^2}. \tag{38}$$

The current density can be calculated from the bulk flow velocity as

$$\mathbf{j} = \sum_s q_s n_s \mathbf{V}_s, \tag{39}$$

and has components

$$j_x = n_0 e\gamma(u_{xi} - u_{xe})\mathrm{sn}(z/L)\mathrm{dn}(z/L), \tag{40}$$

$$j_y = n_0 e(u_{yi} - u_{ye})\mathrm{cn}(z/L)\mathrm{dn}(z/L), \tag{41}$$

$$j_z = 0. \tag{42}$$

Using Eqs. (A11) and (A17), we can show that these expressions are equivalent to those obtained macroscopically from Ampère's law [Eq. (11)].

In the models in e.g., Refs. 1, 38, and 39, the spatial structure of the current density is determined solely by the structure of the bulk flow velocity since the density is constant, in contrast to the classic Harris sheet model,[46] where the bulk flow velocity is constant, and it is the spatial dependence of the density that determines the structure of the current density. In this extended model (and also that of Kolotkov *et al.*[2]), however, both the bulk-flow velocity and density are spatially dependent, and so the spatial structure of the current density is determined from the product of the two quantities.

A. Limiting values of *k*

In the limit $k \to 1$, the number density, temperature, and pressure [Eqs. (29)–(31)] go to the form discussed by Kolotkov *et al.*[2] for the force-free Harris sheet, and the DF (24) becomes the Kolotkov DF (note that our notation is slightly different).

In the limit $k \to 0$, the field becomes linear force-free, and we get a DF of the form

$$f_s = \frac{\gamma^{3/2} n_0 \exp(-\gamma\beta_s H_s)}{\left(\sqrt{2\pi} v_{th,s}\right)^3}\left(\bar{a}_0 - \frac{\gamma^2 u_{xs}^2}{4v_{th,s}^2} + \frac{\gamma}{4}(\gamma\beta_s u_{xs} p_{xs} - \pi)^2\right)$$

$$+\frac{1}{4}\frac{n_0 \exp(-\beta_s H_s)}{\left(\sqrt{2\pi} v_{th,s}\right)^3}\left(4\bar{b}_0 - 2 - \frac{u_{ys}^2}{v_{th,s}^2} + \left(\beta_s u_{ys} p_{ys} + 2\right)^2\right), \tag{43}$$

which is a modified form of the DF obtained in the $k \to 0$ limit of the DF (14). The density and temperature have the form given by Eqs. (29) and (30), respectively, where $\mathrm{sn}(z/L) = \sin(z/L)$.

V. VELOCITY SPACE STRUCTURE OF DF

In this section, we present some illustrative plots of the DF (24) to show the effect of changing γ, i.e., the effect of changing the energy dependence of the different particle populations. In the v_x- and v_y- directions, it is possible to choose sets of parameters for which there are multiple peaks in the DF, which may have implications for the stability of the equilibrium. Neukirch *et al.*[39] and Abraham-Shrauner[1] derive conditions on the parameters in their models such that their DFs will be single-peaked over the whole phase space. Due to the increased complexity of the DFs in terms of energy dependence, however, we have not yet carried out a full analysis of the velocity space structure—this is left for a future investigation.

In the discussion of the plots below, we will refer to the cases where the p_{xs} population is "hotter"/"colder" than the p_{ys} one. This refers to the p_{xs} population having an energy dependence resulting in a "narrower"/"wider" Maxwellian factor in the DF than the p_{ys} one. We note, however, that because the DFs are not purely Maxwellian, the temperature cannot be properly defined in terms of the width of the DF, but the widths of the first and second parts of the DF give us a qualitative measure of the temperature difference between the different populations. This notion of temperature should not be confused with the definition of the temperature given in Eq. (30).

A. v_x-direction

In Fig. 3, we plot the electron DF (24) in the v_x-direction (for $v_y = v_z = 0$) with $\gamma = 1$ (i.e., the Abraham-Shrauner DF). We have chosen a set of parameters for which, at $z = 0$, the DF has a double maximum in v_x (these are the same parameters as in Fig. 2). We note, however, that it is also possible to choose parameters for which the DF has only a single maximum in v_x over the whole phase space, if required (by increasing the density of the background populations appropriately). In Fig. 3, and all subsequent figures in this paper, we normalise the DF to have a maximum value of unity.

Our main aim in this section is to investigate the effect of changing γ on the velocity space structure of the DF. This is why we have chosen parameters that give a double maximum for $\gamma = 1$, since the effect of changing γ is illustrated more clearly in such cases. Figure 4 shows plots of the electron DF for various values of γ which are less than unity. For $\gamma = 0.92$, the double maximum still exists, but has become more slight; for the smaller values of γ shown (0.2 and 0.7), the double maximum has disappeared. In the v_x-direction, the second part of the DF (which does not depend on γ) has the Maxwellian form $g(p_{ys})\exp(-\beta_s H_s)$. For $\gamma < 1$, the p_{xs}-dependent population and the first background one are "hotter" than the p_{ys}-dependent and second background populations, and so the Maxwellian factor $\exp(-\gamma\beta_s H_s)$ (in the

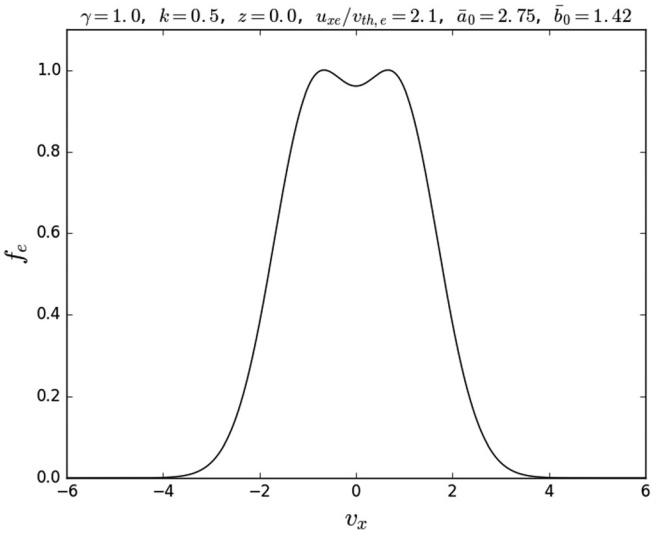

FIG. 3. The electron DF in the v_x-direction (with $v_y = v_z = 0$) for $\gamma = 1$.

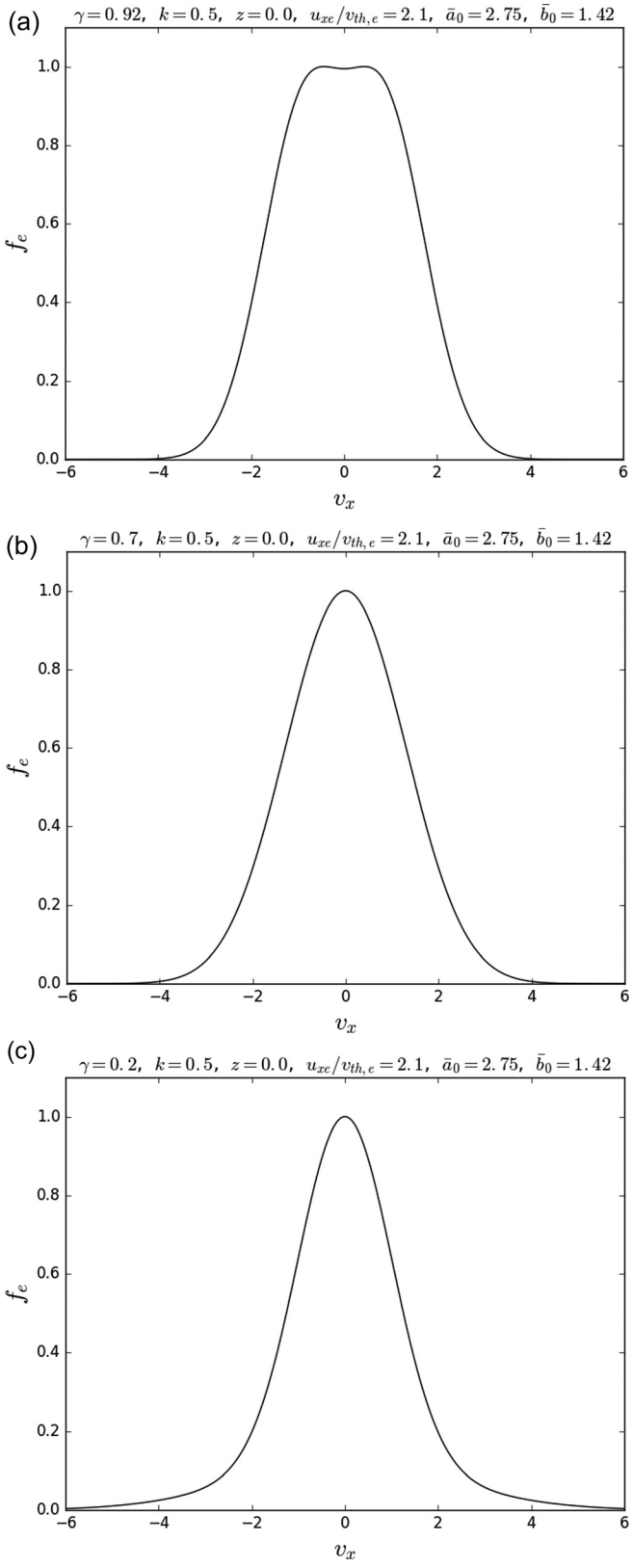

FIG. 4. The electron DF in the v_x-direction (with $v_y = v_z = 0$) for (a) $\gamma = 0.92$, (b) $\gamma = 0.7$, and (c) $\gamma = 0.2$.

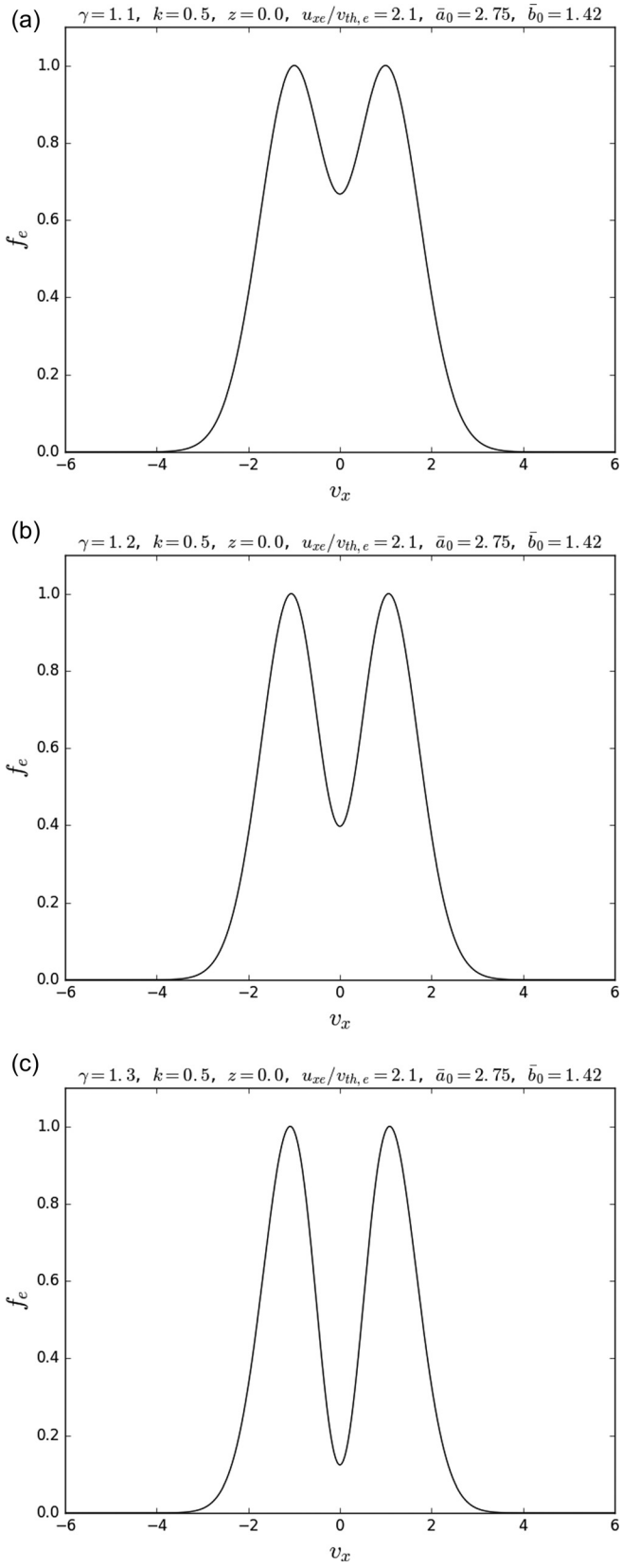

FIG. 5. The electron DF in the v_x-direction (with $v_y = v_z = 0$) for (a) $\gamma = 1.1$, (b) $\gamma = 1.2$, and (c) $\gamma = 1.3$.

first part of the DF) has a narrower width than the factor in the second part of the DF. The "narrow" first part of the DF, including the cosine which can give double maxima in v_x, is therefore "swamped" by the wider second part for decreasing γ, and we see the behaviour in Fig. 4.

Figure 5 shows plots of the electron DF for various values of γ, which are greater than unity. We see that the double maximum in the middle becomes more pronounced as γ is increased. This is due to the fact that the Maxwellian

$\exp(-\gamma\beta_s H_s)$ multiplying the first part of the DF is now wider than the Maxwellian that multiplies the second part (the p_{xs}-dependent population and the first background one are now "colder" than the p_{ys}-dependent and second background populations), so the first part dominates and determines the behaviour of the DF. In Figs. 3–5, we have chosen the parameters $\bar{a}_0$ and $\bar{b}_0$ such that the DFs are positive for all values of γ we consider. As can be seen from the positivity conditions (27), the minimum value of $\bar{a}_0$ becomes significantly larger as γ is increased (for fixed values of the other parameters). If we were to further increase γ, then the central "dip" of the DF would become more pronounced, and the DF would become negative; hence, we would need to increase $\bar{a}_0$ (and adjust $\bar{b}_0$ if required).

B. v_y-direction

In this section, we will show some illustrative plots of the electron DF in the v_y-direction for various values of γ. For the parameter set we used in Figs. 3–5, the DFs are single peaked in all cases except for $\gamma = 1.3$, where there is a double maximum as illustrated in Fig. 6.

From initial investigations, it seems to be difficult to find a set of parameters from which we can illustrate the effect of increasing or decreasing γ. This may be due to the fact that multiple maxima appear to occur at high values of $u_{xe}/v_{th,e}$, for which we require large values of $\bar{a}_0$ to ensure positivity of the DF—i.e., a large background density. This often results in the DF being single-peaked for smaller values of γ.

Possible behaviour of the DF in the v_y-direction can be explored heuristically by noting that, for given values v_x, v_z and z, the DF has the general form

$$f_s(v_y) = C_1 \exp\left(-\frac{\gamma v_y^2}{2v_{th,s}^2}\right) + C_2 \exp\left(-\frac{v_y^2}{2v_{th,s}^2}\right) + C_3 \exp\left(-\frac{(v_y + ku_{ys})^2}{2v_{th,s}^2}\right) + C_4 \exp\left(-\frac{(v_y - ku_{ys})^2}{2v_{th,s}^2}\right), \tag{44}$$

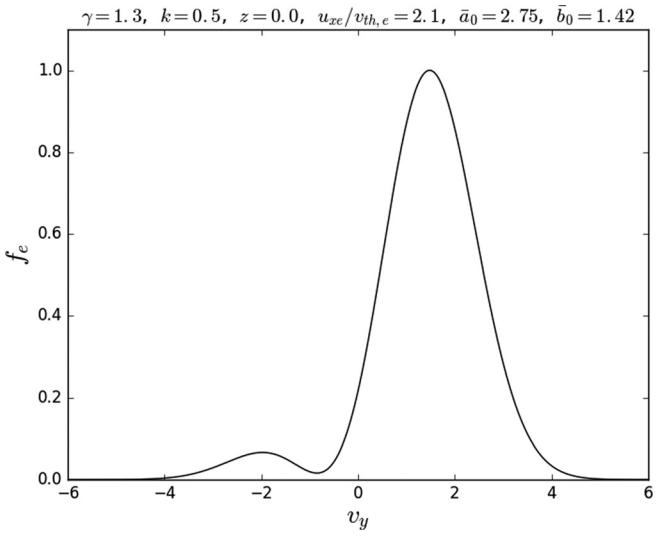

FIG. 6. The electron DF in the v_y-direction (with $v_x = v_z = 0$) for the parameters used in Figure 5(c).

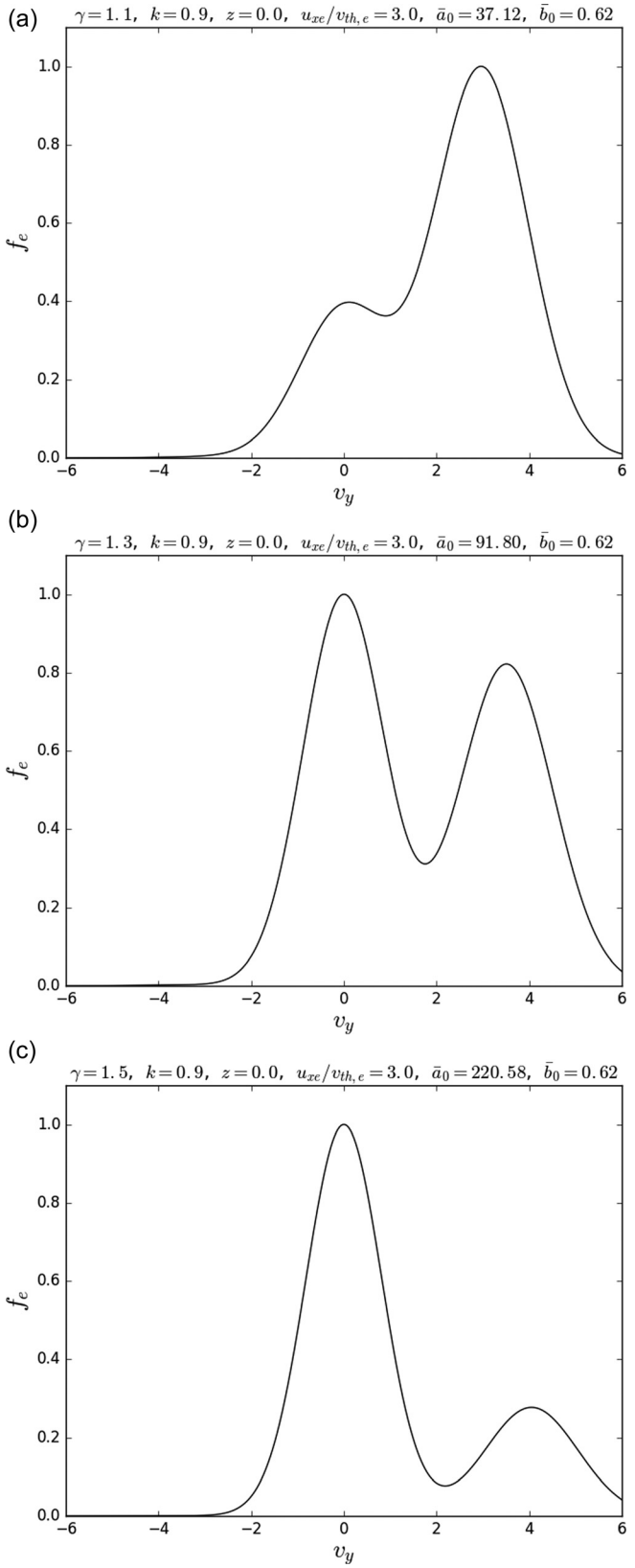

FIG. 7. The electron DF in the v_y-direction (with $v_x = v_z = 0$) for various parameters sets, to give an illustration of the possible behaviour of the DF in this direction.

for constants C_1–C_4, i.e., it consists of two Maxwellian parts with varying widths, and two shifted Maxwellians—one shifted in the positive v_y-direction, and the other in the negative v_y-direction (by the same amount). Depending on the

relative values of C_1–C_4, therefore, the DF can exhibit different behaviour, some examples of which are given in Fig. 7. Note that we have taken different values of $\bar{a}_0$ in each plot, to ensure that the DFs are positive in each case.

VI. SUMMARY

In this paper, we have presented a class of 1D strictly neutral Vlasov-Maxwell equilibrium DFs for both linear and nonlinear force-free current sheets, with magnetic fields defined in terms of Jacobian elliptic functions, which are an extension of the DFs discussed by Abraham-Shrauner[1] to account for non-uniformities in the temperature and density, whilst still maintaining a constant pressure (with respect to the spatial coordinate), as is required for force-balance of the force-free equilibrium. To achieve this, we have used the method of Kolotkov *et al.*,[2] which involves modifying the DF of the original case to include temperature differences between the different particle populations in the model, and then ensuring that strict neutrality is satisfied and that there is consistency between the microscopic and macroscopic parameters of the equilibrium.

The new DF can be regarded as consisting of four particle populations: one depending on p_{xs}, one on p_{ys}, and two background populations. The p_{xs}-dependent and first background population are taken to have the same energy dependence in the DF, as do both the p_{ys}-dependent and second background populations. Note that for the limit of vanishing elliptic modulus, k, to give continuous DFs and pressure, density, and temperature profiles, we require a particular choice of the constants characterising the background populations, but this form can be changed for other k values if desired (it has the "drawback" of giving a very large maximum density for certain parameter values).

We have derived sufficient conditions on the parameters such that the positivity of the DFs is ensured, and have given explicit expressions for the density, temperature, and pressure across the current sheet. Additionally, we have derived the components of the bulk-flow velocity from the DF, to show that the spatial structure of the current density is determined by the product of the spatial structure of the density and bulk-flow velocity, in contrast to the models of, e.g., Abraham-Shrauner[1] and Neukirch *et al.*[39] where the current density structure is determined solely by the structure of the bulk-flow velocity, and also in contrast to the Harris sheet case,[46] where it is determined solely by the density structure.

We have investigated limiting cases of the elliptic modulus, k. For $k \to 1$, the magnetic field becomes that of the force-free Harris sheet, and in this limit, we recover a DF similar to that found by Kolotkov *et al.*[2] for this magnetic field. In the limit $k \to 0$, the magnetic field becomes linear force-free, and in Abraham-Shrauner's case, the DF takes a form which is similar to the one discussed in Refs. 18, 31, and 37, but which is shifted in p_{xs} and p_{ys}. In our extended model, the $k \to 0$ limit simply gives an extension of this shifted DF to include non-uniformity in both the temperature and density.

We have also illustrated graphically the effect of changing the temperature difference between the particle populations in the DF. In the v_x-direction, we found that making the p_{xs} part "colder" than the p_{ys} part can result in rather pronounced double maxima of the DF (due to a cosine term in v_x), but when the p_{xs} part is "hotter," these maxima are less significant, or the DF becomes single peaked. In the v_y-direction, the DF contains two drifting Maxwellians (with the same energy dependence), and two non-drifting Maxwellians (with different energy dependences), and so there is the possibility of double maxima in the DF depending on the relative values of the coefficients of the separate parts.

Double maxima in the DF may lead to velocity space instabilities (e.g., Ref. 47). Due to the increased complexity of the model, however, we have not attempted a systematic study of the velocity space structure, i.e., we have not derived conditions on the parameters such that the DF can be multi-peaked for some z, as has been done by Neukirch *et al.*[39] and Abraham-Shrauner.[1] This is left for a future investigation. We note, however, that it will be possible to choose the density of the background populations large enough such that there are only single maxima of the DF over the whole phase space.

ACKNOWLEDGMENTS

We acknowledge the support of the Science and Technology Facilities Council via the consolidated Grant Nos. ST/K000950/1 and ST/N000609/1 and the doctoral training grant ST/K502327/1 (O.A.), and the Natural Environment Research Council via Grant No. NE/P017274/1 (Rad-Sat) (O.A.). F.W. and T.N. would also like to thank the University of St. Andrews for general financial support.

APPENDIX: PARAMETER RELATIONS

In Sec. IV, by imposing the strict neutrality condition $n_e(A_x, A_y) = n_i(A_x, A_y) = n$, we obtain the relations

$$n_{0e} \exp\left(\frac{u_{xe}^2}{2v_{th,e}^2}\right) = n_{0i} \exp\left(\frac{u_{xi}^2}{2v_{th,i}^2}\right) = n_0, \tag{A1}$$

$$a_{0e} \exp\left(-\frac{u_{xe}^2}{2v_{th,e}^2}\right) = a_{0i} \exp\left(-\frac{u_{xi}^2}{2v_{th,i}^2}\right) = a_0, \tag{A2}$$

$$a_{1e} \exp\left(-\frac{(1+\gamma k^2)u_{xe}^2}{2v_{th,e}^2}\right) = a_{1i} \exp\left(-\frac{(1+\gamma k^2)u_{xi}^2}{2v_{th,i}^2}\right) = a_1, \tag{A3}$$

$$b_{0e} \exp\left(-\frac{u_{xe}^2}{2v_{th,e}^2}\right) = b_{0i} \exp\left(-\frac{u_{xi}^2}{2v_{th,i}^2}\right) = b_0. \tag{A4}$$

$$b_{1e} \exp\left(\frac{k^2u_{ye}^2 - u_{xe}^2}{2v_{th,e}^2}\right) = b_{1i} \exp\left(\frac{k^2u_{yi}^2 - u_{xi}^2}{2v_{th,i}^2}\right) = b_1, \tag{A5}$$

$$b_{2e} \exp\left(\frac{k^2u_{ye}^2 - u_{xe}^2}{2v_{th,e}^2}\right) = b_{2i} \exp\left(\frac{k^2u_{yi}^2 - u_{xi}^2}{2v_{th,i}^2}\right) = b_2, \tag{A6}$$

$$\beta_e|u_{xe}| = \beta_i|u_{xi}|, \tag{A7}$$

$$-\beta_e u_{ye} = \beta_i u_{yi}. \tag{A8}$$

Using the choices (20) and (21) for a_{0s} and b_{0s}, the conditions (A2) and (A4) can equivalently be written as

$$\bar{a}_{0e} \exp\left(-\frac{u_{xe}^2}{2v_{th,e}^2}\right) = \bar{a}_{0i} \exp\left(-\frac{u_{xi}^2}{2v_{th,i}^2}\right) = \bar{a}_0, \tag{A9}$$

$$\bar{b}_{0e} \exp\left(-\frac{u_{xe}^2}{2v_{th,e}^2}\right) = \bar{b}_{0i} \exp\left(-\frac{u_{xi}^2}{2v_{th,i}^2}\right) = \bar{b}_0, \tag{A10}$$

where $a_0 = \bar{a}_0 + \gamma/(2k^2)$, $b_0 = \bar{b}_0 - 1/(2k^2)$.

By calculating two expressions for the pressure P_{zz}, in terms of the macroscopic and microscopic parameters of the equilibrium, respectively, and comparing these expressions, we obtain the relations

$$n_0 \frac{\beta_e + \beta_i}{\beta_e \beta_i} = \frac{B_0^2}{2\mu_0}, \tag{A11}$$

$$\frac{a_0}{\gamma} + b_0 = \frac{P_{t1} + P_{t2}}{B_0^2/2\mu_0} - \frac{3}{2}, \tag{A12}$$

$$\frac{a_1}{\gamma} = -\frac{1}{2k^2}, \tag{A13}$$

$$b_1 = \frac{1}{4}\left(\frac{1}{k} + 1\right)^2, \tag{A14}$$

$$b_2 = \frac{1}{4}\left(\frac{1}{k} - 1\right)^2, \tag{A15}$$

$$\frac{2}{B_0 L} = \gamma \beta_s |u_{xs}| q_s = \beta_s u_{ys} q_s \Rightarrow u_{ys} = \gamma |u_{xs}|. \tag{A16}$$

Similarly to previous work (e.g., Ref. 39), we can derive an expression for the current sheet half-width L, in terms of the microscopic parameters, as

$$L = \left(\frac{2(\beta_e + \beta_i)}{\mu_0 e^2 \beta_e \beta_i n_0 (u_{yi} - u_{ye})^2}\right)^{1/2}. \tag{A17}$$

[1]B. Abraham-Shrauner, "Force-free Jacobian equilibria for Vlasov-Maxwell plasmas," Phys. Plasmas **20**(10), 102117 (2013).
[2]D. Y. Kolotkov, I. Y. Vasko, and V. M. Nakariakov, "Kinetic model of force-free current sheets with non-uniform temperature," Phys. Plasmas **22**(11), 112902 (2015).
[3]N. A. Bobrova and S. I. Syrovatskiĭ, "Violent instability of one-dimensional forceless magnetic field in a rarefied plasma," Sov. J. Exp. Theor. Phys. Lett. **30**, 535 (1979).
[4]M. G. Kivelson and K. K. Khurana, "Models of flux ropes embedded in a Harris neutral sheet: Force-free solutions in low and high beta plasmas," J. Geophys. Res. **100**, 23637–23646, doi:10.1029/95JA01548 (1995).
[5]G. E. Marsh, *Force-Free Magnetic Fields: Solutions, Topology and Applications* (World Scientific, Singapore, 1996).
[6]E. Tassi, F. Pegoraro, and G. Cicogna, "Solutions and symmetries of force-free magnetic fields," Phys. Plasmas **15**(9), 092113 (2008).
[7]E. V. Panov, A. V. Artemyev, R. Nakamura, and W. Baumjohann, "Two types of tangential magnetopause current sheets: Cluster observations and theory," J. Geophys. Res. (Space Phys.) **116**, A12204, doi:10.1029/2011JA016860 (2011).
[8]T. Wiegelmann and T. Sakurai, "Solar force-free magnetic fields," Living Rev. Sol. Phys. **9**(1), 5 (2012); ISSN 1614-4961.
[9]P. Eric, *Magnetohydrodynamics of the Sun* (Cambridge University Press, 2014).
[10]I. Y. Vasko, A. V. Artemyev, A. A. Petrukovich, and H. V. Malova, "Thin current sheets with strong bell-shape guide field: Cluster observations and models with beams," Ann. Geophys. **32**, 1349–1360 (2014).
[11]L. M. Zelenyi, A. G. Frank, A. V. Artemyev, A. A. Petrukovich, and R. Nakamura, "Formation of sub-ion scale filamentary force-free structures in the vicinity of reconnection region," Plasma Phys. Controlled Fusion **58**(5), 054002 (2016).
[12]C. Akcay, W. Daughton, V. S. Lukin, and Y.-H. Liu, "A two-fluid study of oblique tearing modes in a force-free current sheet," Phys. Plasmas **23**(1), 012112 (2016).
[13]D. Burgess, P. W. Gingell, and L. Matteini, "Multiple current sheet systems in the outer heliosphere: Energy release and turbulence," Astrophys. J. **822**, 38 (2016).
[14]A. V. Artemyev, V. Angelopoulos, J. S. Halekas, A. Runov, L. M. Zelenyi, and J. P. McFadden, "Mars's magnetotail: Nature's current sheet laboratory," J. Geophys. Res.: Space Phys. **122**, 5404–5417, doi:10.1002/2017JA024078 (2017); ISSN 2169-9402.J.
[15]A. V. Artemyev, V. Angelopoulos, J. Liu, and A. Runov, "Electron currents supporting the near-Earth magnetotail during current sheet thinning," Geophys. Res. Lett. **44**, 5–11, doi:10.1002/2016GL072011 (2017).
[16]*Reconnection of Magnetic Fields: Magnetohydrodynamics and Collisionless Theory and Observations*, 1st ed., edited by J. Birn and E. R. Priest (Cambridge University Press, 2007), p. 3, ISBN 9780521854207.
[17]F. Wilson, T. Neukirch, M. Hesse, M. G. Harrison, and C. R. Stark, "Particle-in-cell simulations of collisionless magnetic reconnection with a non-uniform guide field," Phys. Plasmas **23**(3), 032302 (2016).
[18]M. G. Harrison and T. Neukirch, "Some remarks on one-dimensional force-free Vlasov-Maxwell equilibria," Phys. Plasmas **16**(2), 022106 (2009).
[19]M. Hesse, M. Kuznetsova, K. Schindler, and J. Birn, "Three-dimensional modeling of electron quasiviscous dissipation in guide-field magnetic reconnection," Phys. Plasmas **12**(10), 100704 (2005).
[20]Y.-H. Liu, W. Daughton, H. Karimabadi, H. Li, and V. Roytershteyn, "Bifurcated structure of the electron diffusion region in three-dimensional magnetic reconnection," Phys. Rev. Lett. **110**, 265004 (2013).
[21]F. Guo, H. Li, W. Daughton, and Y.-H. Liu, "Formation of hard power laws in the energetic particle spectra resulting from relativistic magnetic reconnection," Phys. Rev. Lett. **113**, 155005 (2014).
[22]F. Guo, Y.-H. Liu, W. Daughton, and H. Li, "Particle acceleration and plasma dynamics during magnetic reconnection in the magnetically dominated regime," Astrophys. J. **806**, 167 (2015).
[23]F. Zhou, C. Huang, Q. Lu, J. Xie, and S. Wang, "The evolution of the ion diffusion region during collisionless magnetic reconnection in a force-free current sheet," Phys. Plasmas **22**(9), 092110 (2015).
[24]F. Guo, X. Li, H. Li, W. Daughton, B. Zhang, N. Lloyd-Ronning, Y.-H. Liu, H. Zhang, and W. Deng, "Efficient production of high-energy nonthermal particles during magnetic reconnection in a magnetically dominated ion-electron plasma," Astrophys. J. Lett. **818**, L9 (2016).
[25]F. Guo, H. Li, W. Daughton, X. Li, and Y.-H. Liu, "Particle acceleration during magnetic reconnection in a low-beta pair plasma," Phys. Plasmas **23**(5), 055708 (2016).
[26]F. Fan, C. Huang, Q. Lu, J. Xie, and S. Wang, "The structures of magnetic islands formed during collisionless magnetic reconnections in a force-free current sheet," Phys. Plasmas **23**(11), 112106 (2016).
[27]N. A. Bobrova, S. V. Bulanov, J. I. Sakai, and D. Sugiyama, "Force-free equilibria and reconnection of the magnetic field lines in collisionless plasma configurations," Phys. Plasmas **8**, 759–768 (2001).
[28]K. Nishimura, S. P. Gary, H. Li, and S. A. Colgate, "Magnetic reconnection in a force-free plasma: Simulations of micro- and macroinstabilities," Phys. Plasmas **10**, 347–356 (2003).
[29]K. Bowers and H. Li, "Spectral energy transfer and dissipation of magnetic energy from fluid to kinetic scales," Phys. Rev. Lett. **98**(3), 035002 (2007).
[30]W. Alpers, "Steady state charge neutral models of the magnetopause," Astrophys. Space Sci. **5**, 425–437 (1969).
[31]P. J. Channell, "Exact Vlasov-Maxwell equilibria with sheared magnetic fields," Phys. Fluids **19**, 1541–1545 (1976).
[32]F. Mottez, "Exact nonlinear analytic Vlasov-Maxwell tangential equilibria with arbitrary density and temperature profiles," Phys. Plasmas **10**, 2501–2508 (2003).
[33]O. Allanson, T. Neukirch, S. Troscheit, and F. Wilson, "From one-dimensional fields to Vlasov equilibria: Theory and application of Hermite polynomials," J. Plasma Phys. **82**(3), 905820306 (2016).

[34]E. Moratz and E. W. Richter, "Elektronen-Geschwindigkeitsverteil ungsfunktionen für kraftfreie bzw. teilweise kraftfreie Magnetfelder," Z. Naturforsch., A **21**, 1963 (1966).
[35]A. Sestero, "Self-consistent description of a warm stationary plasma in a uniformly sheared magnetic field," Phys. Fluids **10**, 193–197 (1967).
[36]D. Correa-Restrepo and D. Pfirsch, "Negative-energy waves in an inhomogeneous force-free Vlasov plasma with sheared magnetic field," Phys. Rev. E **47**, 545–563 (1993).
[37]N. Attico and F. Pegoraro, "Periodic equilibria of the Vlasov-Maxwell system," Phys. Plasmas **6**, 767–770 (1999).
[38]M. G. Harrison and T. Neukirch, "One-dimensional Vlasov-Maxwell equilibrium for the force-free Harris sheet," Phys. Rev. Lett. **102**(13), 135003 (2009).
[39]T. Neukirch, F. Wilson, and M. G. Harrison, "A detailed investigation of the properties of a Vlasov-Maxwell equilibrium for the force-free Harris sheet," Phys. Plasmas **16**(12), 122102 (2009).
[40]F. Wilson and T. Neukirch, "A family of one-dimensional Vlasov-Maxwell equilibria for the force-free Harris sheet," Phys. Plasmas **18**, 082108 (2011).
[41]C. R. Stark and T. Neukirch, "Collisionless distribution function for the relativistic force-free Harris sheet," Phys. Plasmas **19**(1), 012115 (2012).
[42]O. Allanson, T. Neukirch, F. Wilson, and S. Troscheit, "An exact collisionless equilibrium for the Force-Free Harris Sheet with low plasma beta," Phys. Plasmas **22**(10), 102116 (2015).
[43]D. Nicolas, B. Gerard, A. Nicolas, D. Jeremy, and R. Laurence, "Asymmetric kinetic equilibria: Generalization of the bas model for rotating magnetic profile and non-zero electric field," Phys. Plasmas **22**(9), 092904 (2015).
[44]*NIST Digital Library of Mathematical Functions*, edited by F. W. J. Olver, A. B. Olde Daalhuis, D. W. Lozier, B. I. Schneider, R. F. Boisvert, C. W. Clark, B. R. Miller, and B. V. Saunders (DLMF, 2016).
[45]P. F. Byrd and M. David Friedman, *Handbook of Elliptic Integrals for Engineers and Scientists* (Springer, Berlin, 2013).
[46]E. G. Harris, "On a plasma sheath separating regions of oppositely directed magnetic field," Nuovo Cimento **23**, 115 (1962).
[47]S. Peter Gary, *Theory of Space Plasma Microinstabilities*, Cambridge Atmospheric and Space Science Series (Cambridge University Press, 2005), ISBN 0521437482.